Time-resolved characterization of a pulsed discharge in a stationary bubble

Time-resolved characterization of a pulsed discharge in a stationary bubble

Patrick Vanraes, Anton Nikiforov, Mario Lessiak, Christophe Leys

Ghent University, Jozef Plateaustraat 22, 9000 Ghent, Belgium

E-mail: `patrick.vanraes@ugent.be`

Abstract. In recent years, plasma generation in water has been proposed for the application of water treatment. The process efficiency is believed to be improved by the introduction of bubbles in the plasma active region. For further optimization, the initiating and developmental mechanisms of plasma inside bubbles need to be understood to a greater extent. In order to meet this necessity, we investigated pulsed electrical discharge inside a stationary bubble in water. This paper deals with the evolution of the discharge and of the bubble shape during discharge, investigated by electrical characterization and fast imaging. Only several microseconds after the application of the voltage pulse, plasma light is observed. Different phases are observed during plasma formation. The plasma is strongest at the bubble surface, causing the surrounding water to evaporate. This leads to both the formation of propagating streamers into the water and the expansion and collapse of the bubble. These observations show that plasma inside a bubble has the strongest activity at the bubble surface, making it attractive for water treatment.

1. Introduction

Plasma in or in contact with water generates high-energetic radicals, ions and molecular species as well as UV radiation and shock waves, which makes it suitable for a wide range of applications like water treatment [1–5]. Plasma has a strong oxidation effect, caused by generated OH radicals and O_3 directly in gas phase and H_2O_2 in water. Therefore, it provides a more versatile and more cost-efficient alternative for existing water treatment techniques like ozonation [6,7]. The investigation and optimization of the chemical effect of plasma with liquid electrodes for water treatment has led to a wide number of papers (see e.g. [8] and references therein) and to the recent industrial implementation of plasma treatment of tertiary-treated wastewater effluent and contaminated groundwater [9].

When plasma is generated inside bubbles in water, the plasma-liquid interface is enlarged and the needed input power is decreased in comparison to discharge in water without bubbles. The introduction of externally generated gas bubbles in the region of discharge is therefore expected to improve the efficiency of plasma chemical processes
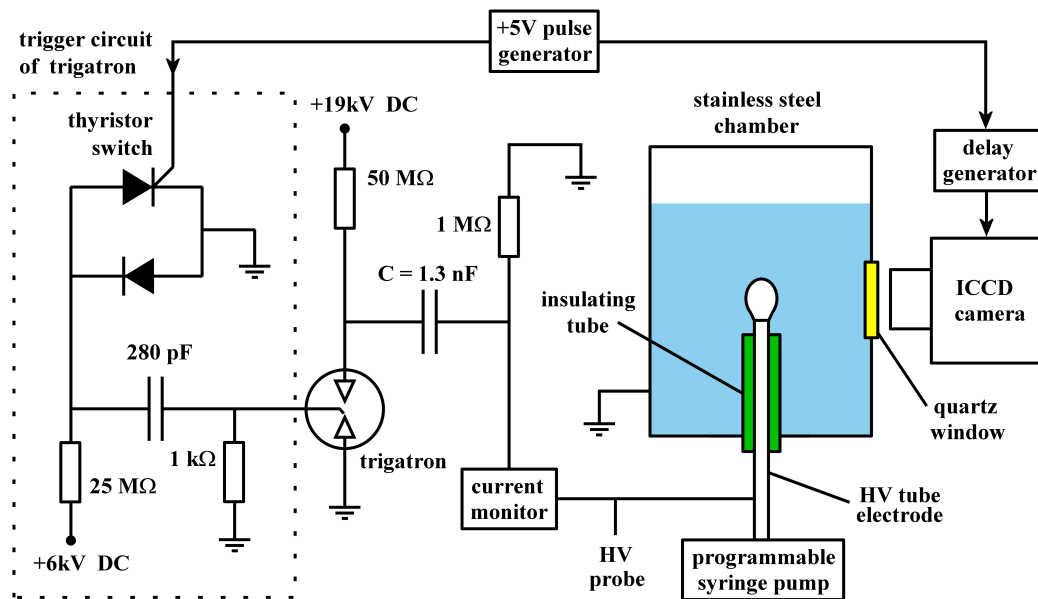
Figure 1. The setup consists of a negative HV pulse generator connected to a metal tube electrode submerged in distilled water inside a stainless steel chamber. A stationary bubble on the metal tube is produced by pumping a gas through the tube with a programmable syringe pump.

at the plasma-liquid interface, where the bubble size and gas flow rate play important roles [7, 10].

The present work deals with pulsed plasma discharge in a stationary bubble on a metal tube electrode in water inside a grounded chamber. Electric characterization and fast-imaging of discharge in helium, argon, nitrogen, oxygen and air bubbles with two different sizes are carried out and compared.

2. Experimental setup and procedure

The electrical bubble discharge is generated inside a grounded cylindrical chamber made of stainless steel with a quartz window of 30 mm diameter, described in [7]. It is filled with distilled water with a conductivity of 22 μS/cm up to 12 cm from the bottom. The stainless steel tube electrode with inner diameter of 0.8 mm and outer diameter of 1.2 mm is submerged vertically in the water with its flattened orifice at the same height as the center of the quartz window. To insulate the tube below its orifice from the water and the chamber, it is placed in a glass tube.

A gas bubble is generated by pumping a gas through the tube electrode with a programmable syringe pump (New Era, model NE-1000). From photographs, the volume of the introduced bubble of 45 μl or 100 μl is determined (corresponding to prolate spheroidal bubbles with a horizontal minor axes length of 2.2 mm or 2.7 mm and a vertical major axis length of 2.3 mm or 3.3 mm respectively). Unless mentioned otherwise, the larger bubble size is used, with helium, argon, nitrogen, oxygen or air as

Table 1. Spectral filters

filter name	λ_{line} (nm)	λ_L (nm)	λ_U (nm)
H_α filter	656	652.5	662.5
O filter	777	770.4	791.0
He filter	588	585.4	595.1
Ar filter	751	747.8	758.2

bubble gas.

A triggered HV power supply with an output capacitance of $C = 1.3$ nF was adjusted to generate negative high voltage (HV) pulses with a rise time of 72 ns, an amplitude of 19 kV and a repetition rate of 0.1 Hz. The schematic of the used power supply and chamber is presented on figure 1. The trigger circuit of the trigatron is controlled by a HTS thyristor switch (Behlke, model 300-100-SCR). The water is grounded in all experiments. Voltage and current waveforms are measured with a Tektronix high voltage probe (model P6015A) and a Pearson current monitor (model 2877) connected to a Tektronix oscilloscope (model DTS 1002).

The discharge is photographed through the circular quartz window with a Hamamatsu ICCD camera (model C8484), with camera exposure times of 50 ns or 5 μs. The camera is triggered with adjustable delay time, using the same trigger signal as the trigger circuit of the trigatron. In some measurements, spectral filters were placed in front of the camera. The lower and upper cutoff wavelengths λ_L and λ_U of the filters are mentioned in table 1, as well as the wavelength λ_{line} of the atomic line the filters were used for.

3. Results

3.1. Electrical characterization

Figure 2 shows the voltage and current waveforms of discharge in an air bubble on two different time scales. The voltage decays exponentially with a time constant of 312 μs. A delay time Δt after the voltage pulse application is determined as the time between the onset of two current pulses. No light emission is observed during this delay time, up to about 100 ns before the second current pulse oscillations start. Therefore, the oscillations indicate the moment of plasma discharge. During one series of experiments, Δt varied with a standard deviation of 0.5 μs. The average value of Δt has an order of magnitude of 10 μs. It is independent of the bubble gas, but decreases with decreasing bubble size. For unprocessed distilled water, for example, Δt has an average value of 12.3 μs and 15.4 μs for bubble volumes of respectively 45 μl and 100 μl.
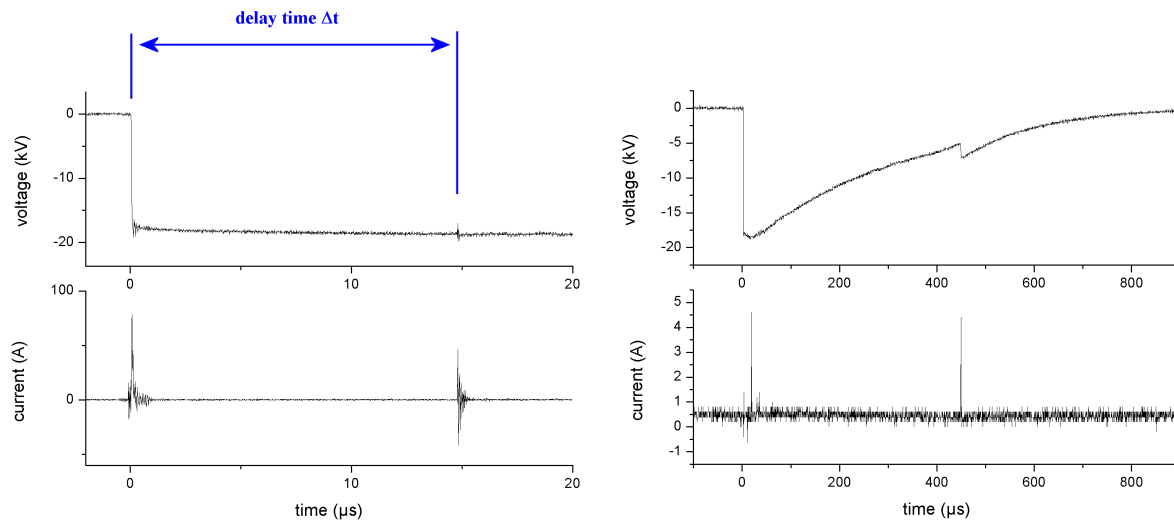
Figure 2. Voltage and current waveforms during discharge in a 100 μl air bubble in distilled water. Oscillations in the waveforms occur a delay time Δt = 14.8 μs after the application of the HV pulse. During the delay time, there was no plasma light emission.

3.2. Time-resolved characterization

An example of the evolution of plasma geometry in the first two microseconds after the delay time Δt is depicted in figure 3. The times indicated on the figure are relative to the point in time where the oscillations on the waveforms begin. Until 100 ns before these oscillations, no plasma light is emitted. Five phases in the development of the plasma geometry are seen. In a time interval of the order of 10 ns or less, 72 ± 18 ns before the voltage oscillations start, intense discharge occurs inside the whole bubble. In a second phase up to 72 ± 30 ns after the start of the oscillations, the plasma diminishes towards the electrode. The third phase is called the *dark phase*, since no emitted light from the bubble bulk is observed during this period of time. Still, plasma remains in proximity of the metal tube. During the fourth phase, the *bubble filling phase*, plasma extends towards the bubble top, either homogeneously for helium bubbles or in filamentary structures along the bubble surface for the other bubble gases. For convenience, these structures are called in short *filaments* henceforth.

The lenght of the dark phase and the bubble filling phase depends strongly on the bubble gas (table 2) and is independent of the bubble size within the accuracy of the measurements. The lenght of the other phases are independent on the bubble gas and size.

From 12.5 ± 2.5 μs after voltage pulse application, the bubble surface blurs due to evaporation of the surrounding water (figure 4). At 22.5 ± 2.5 μs after voltage application, streamer-like structures start to form at the bubble surface, some of which are relatively intense. In order not to confuse these structures with the filaments inside the bubble, they are called henceforth *streamers* in short. The longest streamers that are observed have a branched shape and an estimated velocity with an order of magnitude of
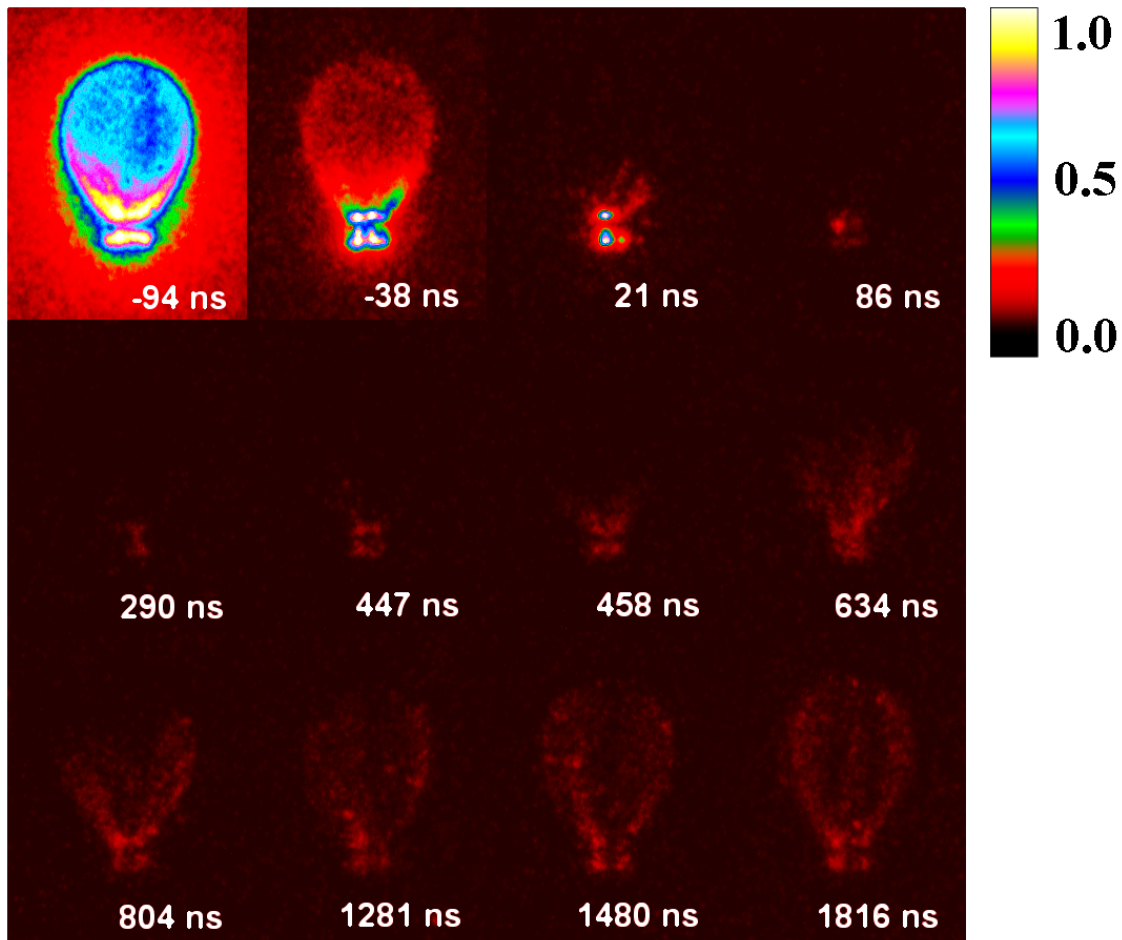
Figure 3. Images of the discharge in a 100 μl air bubble captured by the ICCD camera with an exposure time of 50 ns. Every indicated time is the start time of the camera subtracted from the start time of the voltage oscillations.

Table 2. Phase length

bubble gas	dark phase length (ns)	bubble filling phase length (ns)
helium	176 ± 5	81 ± 21
argon	116 ± 29	80 ± 5
nitrogen	25 ± 17	711 ± 30
oxygen	194 ± 8	196 ± 10
air	394 ± 40	1008 ± 78

10^2 m/s or more. Although the plasma intensity and homogeneity is strongly influenced by the bubble gas, the process of bubble deformation is independent of bubble gas. In bubbles with a volume of 45 μl, streamers are formed at 17.5 ± 2.5 μs after voltage application and they are more intense in comparison to 100 μl bubbles, as seen in figure 5.
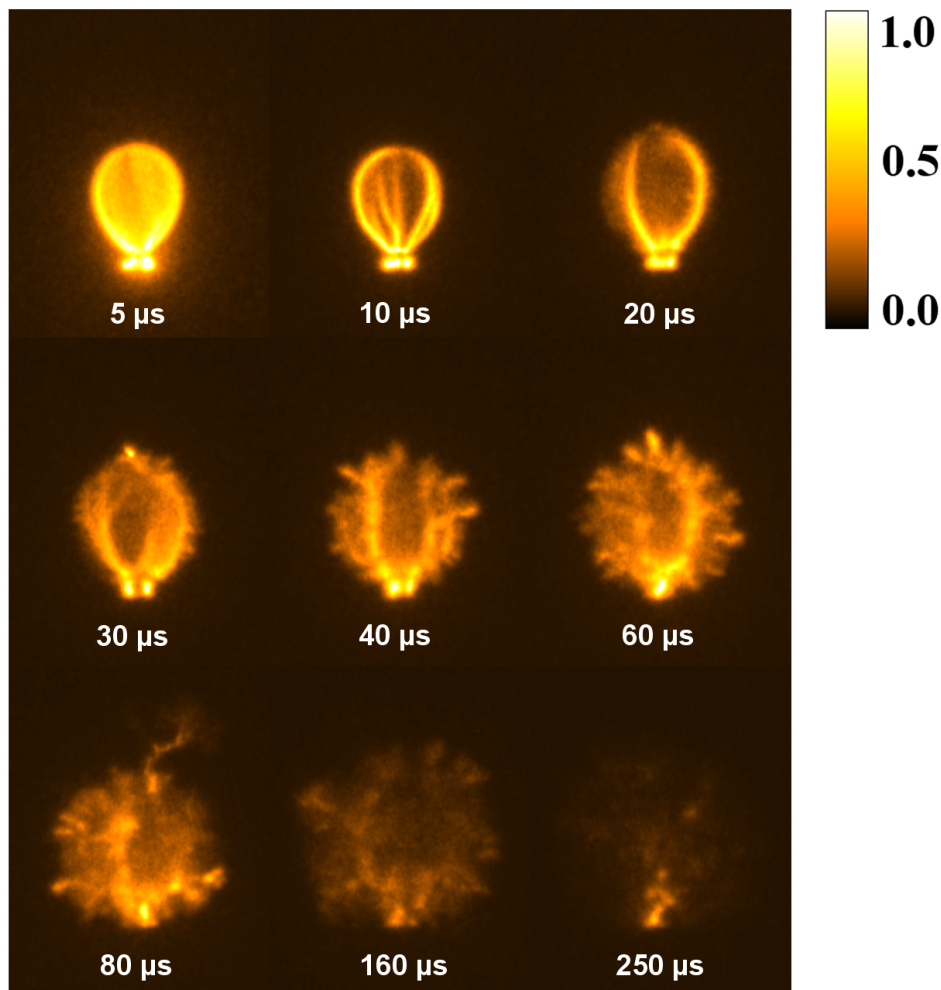
Figure 4. Images of the discharge in a 100 μl air bubble captured by the ICCD camera with an exposure time of 5 mus. The delay time of the camera relative to the time of voltage pulse application is indicated in every image.

The filaments in the bubble emit a spectrum that contains the H_α line, the oxygen line at 777 nm and, for helium and argon bubbles, the corresponding bubble gas element line at 588 nm or 751 nm respectively (figure 6). The filaments in an oxygen bubble are an exception, since H_α is absent or very dim in their spectrum. Relatively far from the bubble surface, H_α is dominant in the streamer spectrum, while the oxygen line and bubble gas element line are absent or very dim.

4. Discussion

The first current peak at the moment of voltage application is caused mostly by displacement current. Also, Joule heating by current from electrolysis contributes to this peak, but this contribution is expected to be very low due to the low water conductivity. Due to the closing of the HTS thyristor switch, a third current peak that corresponds to a negative bump in the voltage waveform is seen more than 400 μs after the voltage
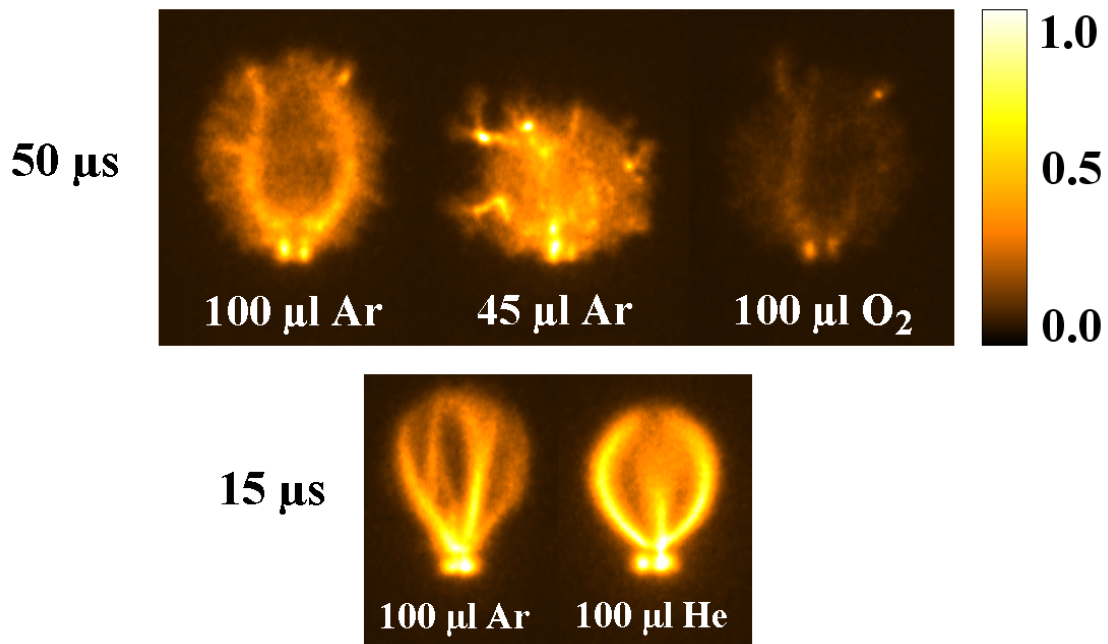
Figure 5. Images of the discharge in a bubble captured by the ICCD camera with an exposure time of 5 μs and a delay time of 50 μs (top) or 15 μs (bottom) relative to the time of voltage pulse application. The bubble gas and size are indicated in every image.
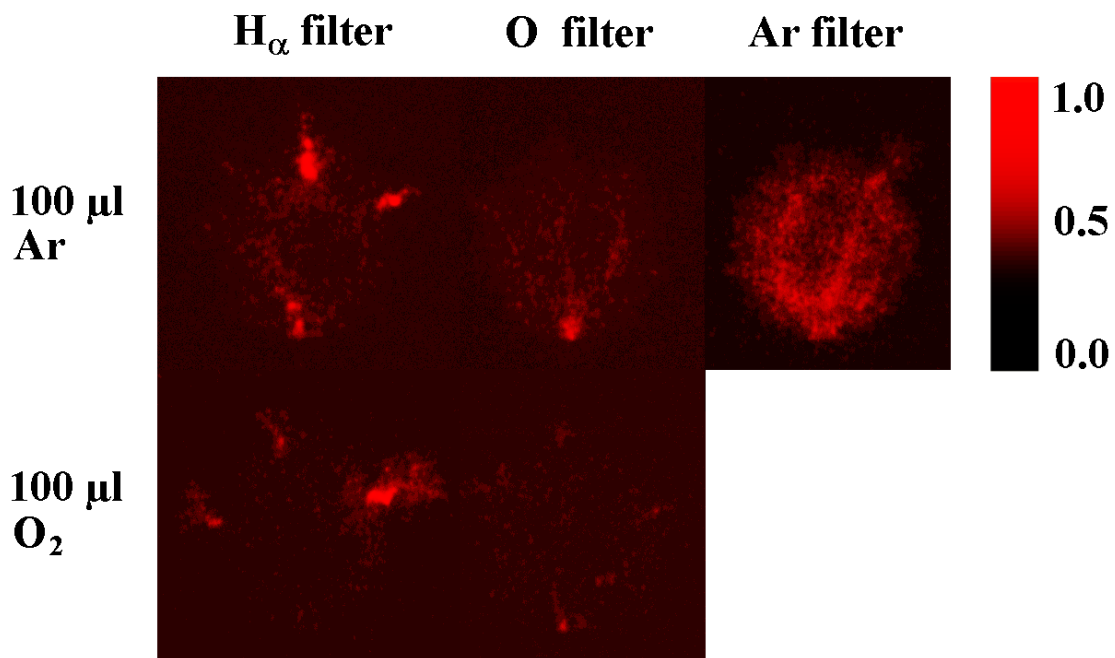

Figure 6. Images of the discharge in a 100 μl argon (top) or oxygen (bottom) bubble captured by the ICCD camera with an exposure time of 5 μs and a delay time of 60 μs relative to the time of voltage pulse application when a spectral filter was placed in front of the camera. The type of spectral filter is indicated above the image.

pulse application. Light emission is no longer observed when this peak occurs, indicating that it is not related to plasma discharge in water.

Plasma light is observed only after a delay time Δt of the order of 10 μs, which indicates that the electric field in the bubble is too small for discharge to occur during this period. The delay time is long enough for ions and dipolar molecules in the water in proximity of the bubble to reorganize. Under the influence of the electric field, a positive net charge accumulates on the bubble surface, enhancing the electric field in the bubble. Once the electric field reaches the critical value necessary for breakdown in the bubble, the first phase of plasma development begins. During the first phase, the bubble is filled with plasma in a time of the order of 10 ns or less, which is too short for atomic and molecular species to travel distances of the order of millimeters. Therefore, the mechanism behind plasma onset is explained by electron avalanches.

The charge accumulation on the bubble surface points out that a capacitive feature of the bubble has to be taken into account. This can also explain the next phases in the development of the plasma geometry. In the first phase, electrons from the HV electrode reach the bubble surface, which leads to the neutralization of the positive net charge and, subsequently, the accumulation of a negative net charge. The electric field in the bulk of the bubble drops rapidly, by which the plasma diminishes towards the electrode. During the dark phase, the negative ions at the bubble surface travel away from the bubble by the repulsive Lorentz force caused by the negative high voltage electrode. The electric field inside the bubble increases, leading to the bubble filling phase.

If we consider the bubble, the surrounding water and the external pulse circuit as a series RC circuit with constant resistance, the difference in average delay time Δt for bubbles of 45 μl and 100 μl can be explained. On the assumption that a prolate spherical bubble with horizontal axes length r and vertical axis length d can be modelled as a classic capacitor that consists of two parallel conductive plates with surface $A \propto r^2$ separated by a distance d by the bubble gas with permittivity $\epsilon \approx \epsilon_0$, its capacitance can be written as

$$C = \epsilon \frac{A}{d} \propto \frac{r^2}{d} \tag{1}$$

Therefore, the time constant $\tau = RC$ is directly proportional to

$$\tau \propto \frac{r^2}{d} \tag{2}$$

Breakdown in the bubble occurs when the electric field E in the bubble gas reaches a critical value E_c. For a charging plate capacitor in a RC circuit, the critical electric field is given by

$$E_c = \frac{V_c}{d} = \frac{V_0 \left(1 - e^{-t/\tau}\right)}{d} \tag{3}$$

where V_c is the critical voltage over the capacitor, V_0 is the constant voltage over the RC circuit and t is the time needed to charge the capacitor up to the critical voltage.

Denoting the parameters of a 45 μl and 100 μl bubble respectively with an index 1 and 2 and equating the critical electric field for both bubble sizes leads to

$$-\frac{t_2}{\tau_2} = \ln\left(1 - \frac{d_2}{d_1}\left(1 - e^{-t_1/\tau_1}\right)\right) \tag{4}$$

On the assumption that $t_1 \ll \tau_1$ and applying the approximations $\ln(1-x) \approx -x$ and $1 - \exp(-x) \approx x$ for $x \ll 1$, equation 4 is reduced to

$$\frac{t_2}{t_1} = \frac{d_2 \tau_2}{d_1 \tau_1} = \frac{r_2^2}{r_1^2} \tag{5}$$

where equation 2 was used. Substituting the average experimental values of Δt in t_1 and t_2, we find that $t_2/t_1 = 1.25$, which deviates 17.2% from $r_2^2/r_1^2 = 1.51$. Considering the simplicity of the model, this is a good agreement.

The branched structure and the estimated velocity of the streamers in our measurements are in agreement with the lower values mentioned in literature for pulsed streamers in water without externally generated bubbles [11–14]. Also, typical spectra of pulsed streamer discharge in water contain a strong H_α line and a weak oxygen line at 777 nm, which indicates that the streamers in our measurements are similar in nature [12, 14].

5. Conclusion

Plasma light emission is recorded only a delay time Δt of the order of 10 μs after the HV pulse application. The plasma geometry evolves in five phases. First, plasma rapidly fills the whole bubble. Next, the plasma decays in 144 ± 35 ns and a dark phase follows. Subsequently, during the bubble filling phase, the plasma extends again towards the top of the bubble. The length of the dark phase and the bubble filling phase depends strongly on the bubble gas. After 22.5 ± 2.5 μs, branching streamer-like structures start to propagate from the bubble surface into the water. Their spectrum contains a strong H_α line and a weak or absent oxygen line at 777 nm.

The delay time Δt and the five phases in the plasma geometry evolution are explained by a capacitive feature of the bubble. A simple model that considers the bubble as a classic plate capacitor is in relatively good agreement with the experimental values in our experiments. The investigated features of the streamers in our measurements resemble the features of pulsed streamer discharge in water, indicating they are similar in nature.

In future research, the electron density and temperature and the plasma chemistry need to be investigated with time-resolved spectroscopy, in order to gain better insight in the time-resolved characterization of a pulsed discharge in a bubble.

References

[1] Kurahashi M, Katsura S and Mizuno A 1997 *Journal of Electrostatics* **42** 93–105

[2] Sunka P, Babicky V, Clupek M, Lukes P, Simek M, Schmidt J and Cernak M 1999 *Plasma Sources Science & Technology* **8** 258–265

[3] Miichi T, Hayashi N, Ihara S, Satoh S and Yamabe C 2002 *Ozone-Science & Engineering* **24** 471–477

[4] Yamatake A, Katayama H, Yasuoka K and Ishii S 2007 *International Journal of Plasma Environmental Science & Technology* **1**

[5] Sato K, Yasuoka K and Ishii S 2010 *Electrical Engineering in Japan* **170** 1–7

[6] Ihara S, Miichi T, Satoh S, Yamabe C and Sakai E 1999 *Japanese Journal of Applied Physics Part 1-Regular Papers Short Notes & Review Papers* **38** 4601–4604

[7] Vanraes P, Nikiforov A and Leys C 2012 *Journal of Physics D-Applied Physics* **45** 245206

[8] Malik M A 2010 *Plasma Chemistry and Plasma Processing* **30** 21–31

[9] Even-Ezra I, Mizrahi A, Gerrity D, Snyder S, Salveson A and Lahav O 2009 *Desalination and Water Treatment* **11** 236–244

[10] Aoki H, Kitano K and Hamaguchi S 2008 *Plasma Sources Science & Technology* **17** 025006

[11] Beroual A, Zahn M, Badent A, Kist K, Schwabe A J, Yamashita H, Yamazawa K, Danikas M, Chadband W G and Torshin Y 1998 *IEEE Electrical Insulation Magazine* **14** 6–17

[12] Akiyama H 2000 *Ieee Transactions on Dielectrics and Electrical Insulation* **7** 646–653

[13] van Veldhuizen E and Rutgers W 2001 *15th International Symposium on Plasma Chemistry* 3245–3250

[14] An W, Baumung K and Bluhm H 2007 *Journal of Applied Physics* **101**